

Nonlinear generation of the fundamental and first harmonic of a periodic surface profile under the action of *s*-polarized laser radiation

V. N. Seminogov and A. I. Khudobenko

Center for Scientific Research on Laser Technology, USSR Academy of Sciences

(Submitted 1 February 1989)

Zh. Eksp. Teor. Fiz. **96**, 504–524 (August 1989)

We have developed an analytic nonlinear theory which describes the formation of periodic structures on a surface subjected to *s*-polarized laser radiation. In this paper we investigate the processes by which laser-induced evaporation of material and photochemical etching of semiconductors can generate periodic surface profiles, and rigorously derive dynamic equations which describe the linear and steady-state nonlinear oscillatory regimes for generation of the fundamental and first spatial harmonics of these profiles. We study the relative roles of intermode and intramode nonlinearities, as well as the effect of reactive nonlinearities which are due to interference between the fields of resonance surface electromagnetic waves and those of second-order diffraction. Our work clarifies the importance of topological nonlinearities caused by rescattering of temperature waves or concentration waves of electron-hole pairs by the generated profile. We show that under the action of laser irradiation it is possible to create a profile for which absorption of radiation incident on the surface reaches 100%.

1. INTRODUCTION

The classical problem of reflection of light from a surface with a periodic profile has attracted special interest in recent years. A number of new linear and nonlinear optical phenomena have been discovered,^{1,2} caused by a sharp increase in the local field near the surface due to resonance excitation of surface electromagnetic waves (SEW). In particular, it has been shown that a profile with period on the order of the wavelength of the incident radiation can give rise to total suppression of specular reflection and anomalously high absorption of light³⁻⁶ when the depth of the profile is close to optimal.

At the same time, it has been established theoretically and experimentally that surface periodic structures (SPS) with a period on the order of the wavelength can be induced by light itself (reviewed in Refs. 7–10), due to diffraction of the light by spatial modulations of the profile and interference of the diffracted waves. In light of this, it is natural to ask the following questions: can a significant variation of the specular reflection coefficient be induced during stimulated generation of SPS, and is it possible for laser radiation to create a profile with 100% absorptivity? Of course, these effects would be of great interest, since they imply the possibility of enhanced self-consistent energy injection of radiation into the material mediated by the surface. This type of energy injection should in turn affect the fundamental processes by which laser radiation interacts with matter in a decisive fashion. However, the available data are clearly inadequate to answer these questions. To explain why this is so and give a more detailed statement of the problem, we should say a few words about the state of theory and experiment with regard to SPS.

These profiles are well-studied in their initial stages of development.⁷⁻¹⁰ A linear theory of SPS generation has been developed for the processes of laser evaporation (LE) of material,⁷⁻¹⁰ photochemical etching (PCE) of semiconductors,¹¹⁻¹³ pyrolytic etching and deposition of films on substrates¹³⁻¹⁵; this theory, which uses perturbation methods to calculate the amplitude of the profile modulation $\xi(\mathbf{r}, t)$, predicts that the amplitude of the continuum of resonance

gratings will grow exponentially with time. However, in the case of *s*-polarized radiation (i.e., the electric field intensity vector \mathbf{E}_i is perpendicular to the plane of incidence) one resonance grating will dominate: the one with parameters^{7,10,13}

$$\mathbf{g} \parallel \mathbf{E}_i, \quad g = k_0 \varepsilon_0^{1/2} (n^* - \sin^2 \theta)^{1/2}, \quad n^* = 1 + \varepsilon_0 \frac{(n+m)^2}{(n^2 + m^2)^2}, \quad (1)$$

for *p*-polarized incident waves there are two gratings which dominate:

$$\mathbf{g}_{1,2} \parallel \mathbf{E}_i, \quad g_{1,2} = k_0 \varepsilon_0^{1/2} (n^* \mp \sin \theta), \quad (2)$$

where \mathbf{g} is a reciprocal lattice vector, $g = 2\pi/d$ where d is the grating period, $g_0 = 2\pi/\lambda$, λ is the wavelength in vacuum, $\varepsilon = (n + im)^2$, $\varepsilon_0 > 0$ are the dielectric permittivities of the material and the etchant (for LE in vacuum $\varepsilon_0 = 1$), θ is the angle at which the radiation is incident on the material from the etchant, and E_{it} is the projection of \mathbf{E}_i on the average boundary between the medium.

Experiments show¹⁶⁻²⁴ that as we increase the length of the laser pulse, the number of pulses which arrive, or the energy per pulse, the evolution of the SPS ceases to obey the linear theory and becomes nonlinear. For the case of *s*-polarized pump waves, this results in the generation of a profile made up of both the grating (1) and its first harmonic with wave vector $2\mathbf{g}$, while for a *p*-polarized pump (2) is accompanied by gratings with the sum and difference spatial periods, i.e., $(\mathbf{g}_1 \pm \mathbf{g}_2)$. SPS with profiles whose Fourier spectra are even more complex have been recorded,^{21,22,24} e.g., structures of Bénard-cell type.²² In addition, several experimenters^{23,25-28} have reported observing considerable variations in the reflectivity and absorptivity of metals under the action of powerful radiation pulses, which cannot be explained by a dependence of the optical constants of the metal on temperature.²⁷ However, it should be kept in mind that none of the experiments done up to now provide enough information for a complete description of the time evolution of the profile in the nonlinear epoch; likewise, none of these

experiments reliably establishes a connection between the absorptivity of the surface and the parameters of the generated profile.

As for the theory of nonlinear SPS generation, only the first steps have been taken in this area: the investigations in Refs. 29–35 comprise the whole of the theoretical effort to date. It is, of course, obvious that thermal, hydrodynamic or electrodynamic nonlinearities, where the last is due to the nonlinear dependence of the amplitudes of the diffracted waves on the modulation depth of the generated profile, could all cause the amplitude to saturate in the nonlinear epoch. Taking these nonlinearities into account produces a whole class of problems involving the nonlinear dynamics of the Fourier amplitudes of the surface waves and the nonlinear generation of an electromagnetic field with a spectrum of spatial frequencies.

The evolution of a surface profile during LE was investigated in Refs. 29 and 31–35, while the authors of Ref. 30 studied the profile evolution during laser excitation of surface capillary waves. The authors of Refs. 29–31 and 33–35 took into consideration only the electrodynamic nonlinearity. In this regard the treatment given in Ref. 32 is exceptional: its authors also investigated the role of thermal nonlinearities which arise because of the nonlinear Arrhenius dependence of the LE velocity on temperature. The concepts of intramode and intermode electrodynamic nonlinearities were introduced in Ref. 30. The intermode nonlinearity arises because of rescattering of one resonance SEW into another, e.g., by the gratings $2g$ or $g_1 + g_2$, and is found to be important for profile depths $g\xi_{2g} \gtrsim \beta_n$ (Ref. 29), where $\beta_n = \varepsilon_0^{1/2} n / (m^2 + n^2) \ll 1$. The intramode nonlinearity is connected with rescattering of a resonance SEW into either a nonresonant radiated wave or a surface wave by gratings (1) and (2), and is important at depths $g\xi_g \approx \beta_n^{1/2}$ (Ref. 30). In Refs. 29, 34, 35 the case of s -polarized incident radiation was investigated by taking into account only the intermode nonlinearity. However, the results of these papers do not agree among themselves: Ref. 35 predicts a growth in the amplitudes ξ_g and ξ_{2g} which is monotonic in time, whereas Ref. 34 finds a growth regime of ξ_g , ξ_{2g} which is oscillatory, although the amplitude ξ_g for the fundamental grating is found to be unbounded in time.

According to Ref. 30, the growth of the fundamental grating amplitude eventually saturates because of the intramode nonlinearity. In view of this, an investigation of the time evolution of the profile up to a level $g\xi_g \approx \beta_n^{1/2}$ must simultaneously take into account both types of electromagnetic nonlinearity, as was done in Refs. 31, 32. In constructing their theory, the authors of Ref. 33 used an approximate analytic solution to the diffraction problem (based on Rayleigh's hypothesis) for the case of p -polarized incident radiation. In Ref. 31 the problem of diffraction for the case of a normally-incident pump wave was solved numerically based on an integrodifferential equation obtained without using Rayleigh's hypothesis. According to the results of Ref. 33, the profile evolution involves out of phase oscillations of the amplitudes ξ_{g1} , ξ_{g2} and $\xi_{g_1 + g_2}$ [see (2)]. In contrast to Ref. 33, the results of Ref. 31 predict that the temporal dynamics of the profile are not oscillatory: after some transient variations the quasistationary amplitudes $\xi_{2g} \approx \text{const}$ and $\xi_g \approx 0$ [see (1), (2) for $\theta = 0^\circ$] are established. The reason for this disagreement in the conclusions of Refs. 31, 33, 34, 35 re-

mains unclear; equally unclear is the question of whether the absorptivity of the surface can vary significantly during the time evolution of the resonance gratings (1) or (2).

In this article we will develop an analytic nonlinear theory of SPS formation during LE and PCE of a surface. These processes are mediated by pulsed and CW s -polarized laser radiation incident on the surface at an arbitrary incident angle θ ; our theory will be valid until $g\xi_g \approx \beta_n^{1/2}$. We will obtain an analytic solution to the problem of diffraction of light by the emerging profile, taking into account both the intramode and intermode electrodynamic nonlinearities. For the LE and PCE processes we will rigorously derive equations which describe the linear and oscillatory nonlinear stages of generation of the surface profile, including its fundamental and first spatial harmonic. For the first time we elucidate the important role played by "topological" nonlinearities caused by rescattering of temperature waves (for LE) and concentration waves of electron-hole pairs (for PCE) by the generated profile. We take into account the effect of "reactive" nonlinearities which arise because of rescattering of a SEW into the second-order diffracted component of a nonresonant surface wave and subsequent mutual interference of these wave fields. We also identify the role of diffraction "seeds" which are evolving in time and which are created when third-order surface waves interfere with resonant SEWs and second-order diffraction. We investigate the time evolution of the reflectivity and absorptivity of the surface, and show that laser irradiation can in fact create a profile which gives rise to total suppression of specular reflection and 100% absorption of the radiation incident on the surface.

2. DIFFRACTION OF s -POLARIZED WAVES BY A SURFACE WITH A PERIODIC PROFILE: INTERMODE, INTRAMODE, AND REACTIVE NONLINEARITIES

Let us assume that a medium with dielectric permittivity $\varepsilon = (n + im)^2$ occupies the half-space $z' > \xi(x, t)$ and a second medium (i.e., an etchant with $\varepsilon_0 > 0$) occupies the half-space $z' < \xi(x, t)$. Suppose that a plane s -polarized electromagnetic wave is incident on the boundary from the etchant side (the plane of incidence is yz' and the vector \mathbf{E}_i is directed along the x -axis):

$$\mathbf{E}_i(x, y, z', t) = \mathbf{E}_i \exp(ik_y y + ik_z z' - i\omega t) + \text{c.c.}, \quad (3)$$

where $k_x = k_0 \varepsilon_0^{1/2} \sin \theta$ and $k_z = k_0 \varepsilon_0^{1/2} \cos \theta$ are the projections of the vector $\varepsilon_0^{1/2} \mathbf{k}_0$ ($k_0 = \omega/c$) of the incident wave on the y and z' axes, and θ is the angle of incidence of the wave.

In LE and PCE a fundamental grating is generated with the parameters (1), along with its first harmonic. Therefore we will assume that

$$\xi(x, t) = \xi_g(t) e^{-igx} + \xi_{2g}(t) e^{-i2gx} + \xi_{3g} e^{-i3gx} + \text{c.c.}, \quad (4)$$

where $\mathbf{r} = \{x, y\}$ and the vector \mathbf{g} is directed along the x -axis (see Fig. 1). The amplitude ξ_{3g} is due to the initial roughness of the surface; it is small and time-independent, and we will need it later to describe the diffraction "seeds" which are found to affect the dynamics of formation of the profile.

Let us write the field distribution in the region $z' < \xi(x, t)$ (i.e., in the etchant), which arises as a result of the diffraction of the wave (3) by the profile (4), in the form

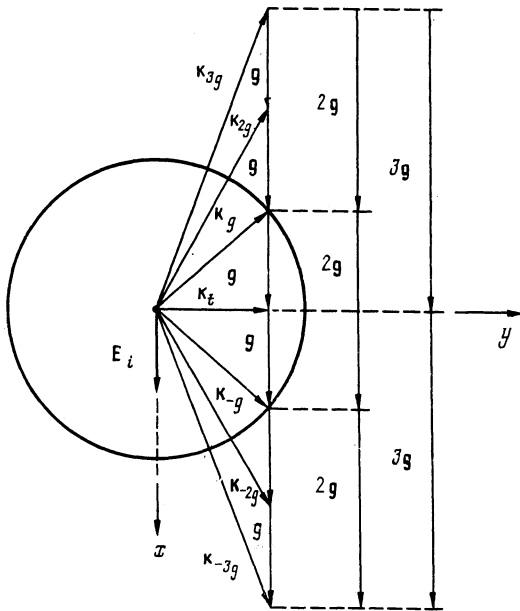


FIG. 1. Rescattering diagram arising from the profile (4) (viewed at the surface from the medium side). The plane of the incident laser wave is $z'y$. The radius of the circle is $\approx k_0 \epsilon_0^{1/2}$. The rescattering of the incident k_i wave by the grating g generates two resonance $k_{\pm g}$ waves. The rescattering between the resonant k_g and k_{-g} waves results in a grating $2g$. The nonresonant surface $k_{\pm 2g}$ waves arise as a result of scattering of the k_i wave by the grating $2g$ and the $k_{\pm g}$ wave by the grating g . The nonresonant surface $k_{\pm 3g}$ waves are generated because of rescattering of the k_i wave by the grating $3g$, the $k_{\pm g}$ wave by the grating $2g$, and the $k_{\pm 2g}$ wave by the grating g .

$$\mathbf{E} = \mathbf{E}_i \exp(ik_y y + ik_z z' - i\omega t)$$

$$+ \sum_p \mathbf{E}_{pg} \exp(ik_{pg} \mathbf{r} + \Gamma_{pg} z' - i\omega t) + \text{c.c.}$$

$$= \mathbf{E}(\omega) e^{-i\omega t} + \text{c.c.}, \quad (5)$$

where $k_{pg} = k_i - pg$, and $p = 0, \pm 1, \dots$, $\Gamma_{pg}^2 = k_{pg}^2 - k_0^2 \epsilon_0$; we have $\text{Re } \Gamma_{pg} > 0$ if $k_{pg} > k_0 \epsilon_0^{1/2}$ and $\text{Im } \Gamma_{pg} < 0$ if $k_{pg} < k_0 \epsilon_0^{1/2}$. From diffraction theory (see, e.g., Ref. 6), it follows that those waves for which $k_{pg} \approx k_0 \epsilon_0^{1/2}$ are resonantly excited. In particular, for the case of a profile (4) with parameters (1) two resonant SEWs are excited with vectors k_g and k_{-g} (see Fig. 1).

The problem of calculating the amplitudes E_{pg} for an arbitrary periodic profile in the presence of resonant diffracted waves, for $|\epsilon| \gg \epsilon_0, k_0 \epsilon_0^{1/2} \xi(x, t) \ll 1$, was solved in Ref. 6. In the case of interest to us, i.e., waves (3) diffracted by the profile (4), the amplitudes of the specularly reflected wave E_{0x} and the resonant waves $E_{\pm gz}$ are determined by solving the system of equations (22), (23) of Ref. 6, which in the present case have the form

$$E_{0x} = (k_z - i\gamma) E_{ix} / (k_z + i\gamma) - ig E_{gz} \xi_g^* + ig E_{-gz} \xi_g, \quad E_{0y} = E_{0z} = 0,$$

$$T_0 E_{gz} = k_z g (E_{ix} - E_{0x}) \xi_g - 2g^2 E_{-gz} \xi_{2g}, \quad (6)$$

$$T_0 E_{-gz} = -k_z g (E_i - E_{0x}) \xi_g^* - 2g^2 E_{gz} \xi_{3g}^*,$$

$$T_0 = T_0' - iT_0'' = \Gamma_g - \beta_m \epsilon_0^{1/2} k_0 - g^4 |\xi_g|^2 / \Gamma_{2g}$$

$$- 4g^4 |\xi_{2g}|^2 / \Gamma_{3g} - i\beta_n \epsilon_0^{1/2} k_0,$$

$$\gamma \approx (m - in) k_0, \quad \beta_m = m \epsilon_0^{1/2} / (m^2 + n^2), \quad \beta_n = n \epsilon_0^{1/2} / (m^2 + n^2). \quad (7)$$

We note that the results of Ref. 6, which are valid for the case $\epsilon_0 = 1$, can be generalized to the case $\epsilon_0 \neq 1$ if we make the substitutions $\epsilon \rightarrow \epsilon/\epsilon_0$, $k_0 \rightarrow k_0 \epsilon_0^{1/2}$ in all the equations of Ref. 6. However, according to Eq. (14) of Ref. 6, the amplitudes $E_{\pm gx}$, $E_{\pm gy}$ can be expressed in terms of the amplitudes E_{0x} , $E_{\pm gz}$:

$$E_{gx} = -ig E_{gz} / \gamma - ik_z (E_{ix} - E_{0x}) \xi_g + 2ig E_{-gz} \xi_{2g}, \quad E_{gy} = ik_t E_{gz} / \gamma,$$

$$E_{-gx} = ig E_{-gz} / \gamma - ik_z (E_{ix} - E_{0x}) \xi_g^* - 2ig E_{gz} \xi_{2g}^*, \quad E_{-gy} = ik_t E_{-gz} / \gamma. \quad (8)$$

Solving the system (6)–(8), we obtain for the field components \mathbf{E}_0 , \mathbf{E}_g

$$E_{0x} = \frac{k_z - i\gamma}{k_z + i\gamma} E_{ix} - \frac{4ik_z}{\Delta} [T_0 g^2 |\xi_g|^2 + g^4 (\xi_g^* \xi_{2g} + \xi_g^2 \xi_{2g}^*)] E_{ix},$$

$$E_{0y} = E_{0z} = 0, \quad (9)$$

$$E_{gz} = \frac{2k_z}{\Delta} (T_0 g \xi_g + 2g^3 \xi_g^* \xi_{2g}) E_{ix}, \quad E_{gx} = -i \frac{g^2 + \gamma T_0}{g\gamma} E_{gz},$$

$$E_{gy} = \frac{ik_t}{\gamma} E_{gz}, \quad (10)$$

in this case the resonant denominator Δ in (9), (10) is given by the equation

$$\Delta = T_0^2 - 2ik_z T_0 g^2 |\xi_g|^2 - 4g^4 |\xi_{2g}|^2 - 2ik_z g^4 (\xi_g^* \xi_{2g} + \xi_g^2 \xi_{2g}^*). \quad (11)$$

The field amplitudes \mathbf{E}_{-g} are found from (10) by the substitution

$$g \rightarrow -g \quad (12)$$

both in the coefficients and in the subscripts and using $\xi_{-pg} = \xi_{pg}^*$, $\Gamma_{-pg} = \Gamma_{pg}$.

The amplitudes $E_{\pm 2g}$, $E_{\pm 3g}$ for the nonresonant surface waves are determined from Eq. (20) of Ref. 6 by using Eqs. (9)–(11). The field components for second- and third-order diffraction in the etchant have the form

$$E_{2gx} = ig E_{gz} \xi_g - ik_z (E_{ix} - E_{0x}) \xi_{2g}, \quad E_{2gy} = 0,$$

$$E_{2gz} = -2g^2 E_{gz} \xi_g / \Gamma_{2g} + 2k_z g (E_{ix} - E_{0x}) \xi_{2g} / \Gamma_{2g},$$

$$E_{3gx} \approx 2ig E_{gz} \xi_{2g} - ik_z (E_{ix} - E_{0x}) \xi_{3g}, \quad E_{3gy} = 0, \quad (13)$$

$$E_{3gz} \approx -6g^2 E_{gz} \xi_{2g} / \Gamma_{3g} + 3k_z g (E_{ix} - E_{0x}) \xi_{3g} / \Gamma_{3g}.$$

The amplitudes \mathbf{E}_{-g} , \mathbf{E}_{-3g} are found from (13), taking the substitution (12) into account.

Let us discuss the physical nature of the nonlinear dependence of the amplitude of the diffracted waves on ξ_g and

ξ_{2g} . The terms in parentheses in Eqs. (9)–(11) arise because of our inclusion of the rescattering

$$\mathbf{E}_{\pm g} \xrightarrow{g} \mathbf{E}_0 \xrightarrow{g} \mathbf{E}_{\mp g} \xrightarrow{2g} \mathbf{E}_{\pm g}$$

(see Fig. 1). The third term in (11) appears because of the rescattering

$$\mathbf{E}_{\pm g} \xrightarrow{2g} \mathbf{E}_{\mp g} \xrightarrow{2g} \mathbf{E}_{\pm g}$$

by the grating (2g). The second term in (10) is caused by the rescattering

$$\mathbf{E}_0 \xrightarrow{g} \mathbf{E}_{\pm g} \xrightarrow{2g} \mathbf{E}_{\mp g}.$$

Since all of these nonlinearities are connected with rescattering between the different resonant waves \mathbf{E}_g and \mathbf{E}_{-g} by the 2g grating, we will refer to them as “intermode” nonlinearities. The third and fourth terms in (7) arise because of the rescattering

$$\mathbf{E}_{\pm g} \xrightarrow{g} \mathbf{E}_{\pm 2g} \xrightarrow{g} \mathbf{E}_{\pm g}, \quad \mathbf{E}_{\pm g} \xrightarrow{2g} \mathbf{E}_{\pm 3g} \xrightarrow{2g} \mathbf{E}_{\pm g}$$

by the gratings g and 2g respectively. The second term in (11) takes into account the rescattering

$$\mathbf{E}_{\pm g} \xrightarrow{g} \mathbf{E}_0 \xrightarrow{g} \mathbf{E}_{\pm g}.$$

Because rescattering involves no energy transfer from one resonant wave to another, we will refer to the corresponding nonlinearities as “intramode”. The first two terms in (7) and the last term determine the dispersion law and damping of the resonant waves as they propagate along the plane of the surface. The change in the dispersion law connected with the third and fourth terms in (7) is analogous to amplitude-dependent changes in the resonant frequency of a nonlinear oscillator.

Let us turn now to a calculation of the field within the medium.

According to Ref. 6, the field distribution in the region $z' > \xi(x, t)$ takes the form

$$\begin{aligned} \mathbf{E}' &= \exp\{-\gamma(z' - \xi(x, t)) - i\omega t\} \sum_p \mathbf{E}_{pg}' \exp(ik_p x) \\ &+ \text{c.c.} = \vec{\mathcal{E}} \exp\{-\gamma(z' - \xi(x, t)) - i\omega t\} + \text{c.c.}, \\ \vec{\mathcal{E}} &= \frac{1}{\gamma} [\mathbf{n} \text{rot } \mathbf{E}(\omega)]|_{z'=\xi(x, t)}, \end{aligned} \quad (14)$$

$$\mathbf{n} = \left(-i \frac{\partial \xi}{\partial x} + \mathbf{k} \right) / \left\{ 1 + \left(\frac{\partial \xi}{\partial x} \right)^2 \right\}^{1/2},$$

where \mathbf{i} , \mathbf{k} , \mathbf{n} are unit vectors directed respectively along the x , z' axes and along the normal to the surface; note that \mathbf{n} points into the region $z' > \xi(x, t)$. The field $\mathbf{E}(\omega)$ is given by Eqs. (5) and (7)–(13). As a result of these equations, in the region $z' > \xi(x, t)$ the field components for zero-order diffraction and resonant diffraction of the field are given by

$$E_{0x}' = -\frac{ik_z}{\gamma} (E_{ix} - E_{0x}), \quad E_{0y}' = 0, \quad (15)$$

$$E_{gx}' = -\frac{i}{\gamma} [gE_{gz} + k_z^3 (E_{ix} - E_{0x}) \xi_{3g} \xi_{2g}^*], \quad (16)$$

$$E_{gy}' = \frac{ik_1}{\gamma} [E_{gz} + ig(E_{ix} + E_{0x}) \xi_g + k_z g (E_{ix} - E_{0x}) \xi_{3g} \xi_{2g}^*].$$

The amplitude of the rescattered fields for second- and third-order diffraction in the region $z' > \xi(x, t)$ can be written in the form

$$\begin{aligned} E_{2gx}' &= \frac{ik_z^2}{\gamma} \left[\frac{g}{\Gamma_{2g}} E_{gz} \xi_g - \frac{k_z}{\Gamma_{2g}} (E_{ix} - E_{0x}) \xi_{2g} - i(E_{ix} + E_{0x}) \xi_{2g} \right. \\ &\quad \left. - k_z (E_{ix} - E_{0x}) \xi_{3g} \xi_g^* \right], \\ E_{2gy}' &= -\frac{2ik_1 g}{\gamma} \left[\frac{g}{\Gamma_{2g}} E_{gz} \xi_g - \frac{k_z}{\Gamma_{2g}} (E_{ix} - E_{0x}) \xi_{2g} - i(E_{ix} + E_{0x}) \xi_{2g} \right. \\ &\quad \left. - g (E_{ix} - E_{0x}) \xi_{3g} \xi_g^* \right], \end{aligned} \quad (17)$$

$$\begin{aligned} E_{3gx}' &= \frac{ik_z^2}{\gamma} \left[\frac{2g}{\Gamma_{3g}} E_{gz} \xi_{2g} - \frac{k_z}{\Gamma_{3g}} (E_{ix} - E_{0x}) \xi_{3g} - i(E_{ix} + E_{0x}) \xi_{3g} \right], \\ E_{3gy}' &= -\frac{3ik_1 g}{\gamma} \left[\frac{2g}{\Gamma_{3g}} E_{gz} \xi_{2g} - \frac{k_z}{\Gamma_{3g}} (E_{ix} - E_{0x}) \xi_{3g} \right. \\ &\quad \left. - i(E_{ix} + E_{0x}) \xi_{3g} \right]. \end{aligned}$$

Here we have neglected the z -components of the fields because of their smallness. In Eqs. (16), (17), along with the fundamental resonant contributions [the first terms in (16), (17)] we have included only those nonresonant contributions which we will need below to calculate the diffraction “seeds”, which are proportional to $\xi_{3g} \xi_g^* \xi_{3g} \xi_{2g}^*$, in the dynamic equations for the Fourier amplitudes of the profile.

The energy dissipated in a unit volume per unit time in the region $z' > \xi(x, t)$ equals

$$\begin{aligned} f &= \frac{1}{4\pi} \mathbf{E}' \frac{\partial \mathbf{D}'}{\partial t} = \frac{\omega \varepsilon''}{2\pi} |\vec{\mathcal{E}}|^2 \exp\{-\gamma_0(z' - \xi(x, t))\} \\ &= [f_0 + (f_g e^{-i g x} + f_{2g} e^{-i 2 g x} + \text{c.c.})] \exp\{-\gamma_0(z' - \xi(x, t))\}, \end{aligned} \quad (18)$$

where $\gamma_0 = \gamma + \gamma^*$ and \mathbf{D}' is the electric displacement vector. After substituting the first expression (14) into (18), we obtain

$$\begin{aligned} f_0 &= \frac{\omega \varepsilon''}{2\pi} \sum_{p=0, \pm 1, \pm 2} |\mathbf{E}_{pg}'|^2, \\ f_g &= \frac{\omega \varepsilon''}{2\pi} (\mathbf{E}_0' \cdot \mathbf{E}_g' + \mathbf{E}_0' \cdot \mathbf{E}_{-g}' + \mathbf{E}_g' \cdot \mathbf{E}_{2g}' \\ &\quad + \mathbf{E}_{-g}' \cdot \mathbf{E}_{-2g}' + \mathbf{E}_{2g}' \cdot \mathbf{E}_{3g}' + \mathbf{E}_{-2g}' \cdot \mathbf{E}_{-3g}'), \\ f_{2g} &= \frac{\omega \varepsilon''}{2\pi} (\mathbf{E}_g' \cdot \mathbf{E}_{-g}' + \mathbf{E}_0' \cdot \mathbf{E}_{2g}' \\ &\quad + \mathbf{E}_0' \cdot \mathbf{E}_{-2g}' + \mathbf{E}_g' \cdot \mathbf{E}_{3g}' + \mathbf{E}_{-g}' \cdot \mathbf{E}_{-3g}'). \end{aligned} \quad (19)$$

When calculating f_0 it is sufficient to include only the contributions with $p = 0, \pm 1$, and to save only the resonance terms in Eq. (16). Then

$$\begin{aligned} f_0 &= \frac{2\omega \varepsilon'' k_z^2 |E_{ix}|^2}{\pi |\gamma|^2 |\Delta|^2} \{ |T_0|^4 - 8g^4 (T_0'^2 - T_0'^2) |\xi_{2g}|^2 + 16g^8 |\xi_{3g}|^4 \\ &\quad + 2(g^2 + k_z^2) [g^2 |T_0|^2 |\xi_g|^2 + 4g^6 |\xi_g \xi_{2g}|^2 \\ &\quad + 2g^4 T_0' (\xi_g^* \xi_{2g} + \xi_g^2 \xi_{2g}^*)] \}, \end{aligned} \quad (20)$$

where T_0 and Δ are defined in (7) and (11). Including Eqs. (15)–(17) in (19), the expression for f_g can be cast in the form

$$f_g = \frac{4\omega\varepsilon''k_z^2g|E_{ix}|^2}{\pi|\gamma|^2|\Delta|^2} \left\{ T_0'g\xi_g(|T_0|^2 - 4g^4|\xi_{2g}|^2) + 2g^3\xi_g^*\xi_{2g}(T_0'^2 - T_0'^2 - 4g^4|\xi_{2g}|^2) - g\xi_g \frac{(k_0^2\varepsilon_0 + k_i^2)}{\Gamma_{2g}} [g^2|T_0|^2|\xi_g|^2 + 4g^6|\xi_g\xi_{2g}|^2 + 2g^4T_0'(\xi_g^*\xi_{2g} + \xi_g^2\xi_{2g}^*)] \right\} + f_g^{(3)}. \quad (21)$$

The first two terms in (21) are obtained from the first two terms of (19) for f_{gi} , while the term in square brackets in (21) appears because of the third and fourth terms in (19); in Eqs. (16), (17) we consider only the resonance contributions. In what follows, we will refer to the nonlinearity in ξ_g , ξ_{2g} , which is connected with the terms in the square brackets in (21), as “reactive”. This reactive nonlinearity arises because of the rescattering of the resonance fields $\mathbf{E}'_{\pm g}$ by the grating \mathbf{g} into the surface waves $\mathbf{E}'_{\pm 2g}$ and subsequent interference between these waves. It is easy to see from (19) that the reactive nonlinearity is significant when $|\mathbf{E}'_{\pm 2g}|$ is comparable to or larger than $|\mathbf{E}'_0|$. In the case of grating (1), it follows from (21) that this will happen when $g|\xi_g| \gtrsim \beta_n^{1/2}$. For small values of $|\xi_g|$ and $|\xi_{2g}|$, the first term in (21) is the important one.

Let us write the amplitude of the first harmonic f_{2g} in the form

$$f_{2g} = \frac{2\omega\varepsilon''k_z^2(g^2 - k_i^2)|E_{ix}|^2}{\pi|\gamma|^2|\Delta|^2} \left\{ g^2|T_0|^2|\xi_g^2 + 4g^4T_0'|\xi_g|^2\xi_{2g} + 4g^6\xi_g^*\xi_{2g}^2 \right\} + f_{2g}^{(3)}. \quad (22)$$

The first three terms in (22) are determined by the first term in (19) when only the resonance contribution to (16) is included. The diffraction “seeds” $f_g^{(3)}$, which are $\sim \xi_{3g}\xi_{2g}^*$ are obtained from the first, second, fifth and sixth terms for f_g in (19), while the diffraction “seeds” $f_{2g}^{(3)} \sim \xi_{3g}\xi_g^*$ are found from the second, third, fourth, and fifth terms in Eq. (19) for f_{2g} . These diffraction “seeds”, as we will see below, are important as $|\xi_g| \rightarrow 0$ or as $|\xi_{2g}| \rightarrow 0$. Therefore, so as to avoid cumbersome expressions as $|\xi_g| \rightarrow 0$, we will use the following approximation in (9) to calculate them:

$$E_{0x} \approx (k_z - i\gamma)E_{ix}/(k_z + i\gamma).$$

As $|\xi_{2g}| \rightarrow 0$ the expressions for E_{0x} in (9) and E_{gz} in (10) can be cast in the form

$$E_{0x} \approx (k_z - i\gamma)E_{ix}/(k_z + i\gamma) - 4ik_zT_0g^2|\xi_g|^2E_{ix}/\Delta,$$

$$E_{gz} = 2k_zT_0g\xi_gE_{ix}/\Delta.$$

As a result,

$$f_g^{(3)} = \frac{4\omega\varepsilon''k_z^2}{\pi|k_z + i\gamma|^2} |E_{ix}|^2 \left(k_z^2 + \frac{k_z^4 + 6k_i^2g^2}{\Gamma_{2g}\Gamma_{3g}} \right) \xi_{3g}\xi_{2g}^*,$$

$$f_{2g}^{(3)} = \frac{4\omega\varepsilon''k_z^2g^2}{\pi|k_z + i\gamma|^2} |E_{ix}|^2 \times \left[\frac{(1 + 2\sin\theta)(T_0'/\Gamma_{3g} + 2g^2|\xi_g|^2) + 1}{|T_0|^2 + 4g^2|\xi_g|^2 \cos\theta(T_0'' + \cos\theta g^2|\xi_g|^2)} \right] \xi_{3g}\xi_g^*. \quad (23)$$

3. PHYSICAL MECHANISM OF PROFILE FORMATION; EQUATIONS FOR THE TIME EVOLUTION OF THE SPS; TOPOLOGICAL NONLINEARITIES

a. Let us first investigate the process of generation of SPS in PCE of semiconductors. Assume that radiation from a CW laser is incident on the surface of the semiconductor (for definiteness we pick n -type GaAs and the etchant $\text{H}_2\text{SO}_4:\text{H}_2\text{O}_2:\text{H}_2\text{O}$), and that the energy quanta of this radiation are larger than the width of the forbidden gap. As a result of diffraction of the light by the initial surface roughness and interference between the diffracted fields near the surface, a spatially-inhomogeneous distribution of electron-hole pairs is generated. Since the rate of etching is proportional to the concentration of minority charge carriers (see Ref. 13 and the citations therein), the surface profile becomes unstable; this is because the amplitudes of the diffracted fields increase as the “seed” roughness gets deeper.

As a consequence of the PCE, the plane which defines the average “boundary” between the semiconductor and the etchant moves as a whole along the z'' axis with velocity $v_0(t)$. Then in the moving coordinate system, x, y, z' connected with the nonmoving coordinate system x, y, z'' by the relation

$$z' = z'' - \int_0^t v_0(\tau) d\tau,$$

the profile of the surface is given by Eq. (4), while the total velocity of the boundary motion is determined by the expression

$$v_z(t) = v_0(t) + \frac{\partial \xi(x, t)}{\partial t} = \beta n(x, z' = \xi(x, t), t),$$

where the constant β is found by using the experimental data. After transforming to a system of coordinates $x, y, z = z' - \xi(x, t)$ in which the boundary is planar, and taking into account (18), (20)–(23), the space-time distribution of the minority carriers (holes) in the bulk semiconductor is determined by the following problem:

$$\frac{\partial n}{\partial t} - v_0 \frac{\partial n}{\partial z} = D \left\{ \frac{\partial^2 n}{\partial x^2} + \left[1 + \left(\frac{\partial \xi}{\partial x} \right)^2 \right] \frac{\partial^2 n}{\partial z^2} - 2 \frac{\partial \xi}{\partial x} \frac{\partial^2 n}{\partial x \partial z} - \left[\frac{\partial^2 \xi}{\partial x^2} - \frac{\partial \xi}{\partial t} \right] \frac{\partial n}{\partial z} \right\} - n/\tau + k[f_0 + (f_g e^{-igx} + f_{2g} e^{-i2gx} + \text{c.c.})] e^{-\gamma_0 z}, \quad (24)$$

$$n(x, z = \infty, t) = n(x, z, t = 0) = 0,$$

$$\left\{ 1 + \left(\frac{\partial \xi}{\partial x} \right)^2 \right\}^{-1/2} \left\{ \left[1 + \left(\frac{\partial \xi}{\partial x} \right)^2 \right] \frac{\partial n}{\partial z} - \frac{\partial \xi}{\partial x} \frac{\partial n}{\partial x} \right\}_{z=0} = \frac{SN}{D} \left(v_0 + \frac{\partial \xi}{\partial t} \right), \quad v_z(t) = v_0(t) + \frac{\partial \xi(x, t)}{\partial t} = \beta n(x, z = 0, t), \quad (25)$$

where γ_0 is defined in (18), n is the number of holes per unit volume, D is the diffusion coefficient, τ is the effective lifetime of the holes, $k = \eta/\hbar\omega$, η is the quantum efficiency, S is the number of holes required to eject one semiconductor atom from the surface into the etchant, and N is the number of semiconductor atoms per unit volume.

In PCE, the characteristic velocity $v_0 = 10^{-7} - 10^{-5}$ cm/sec.¹³ Therefore the conditions $v_0 \ll Dg$, $D/1$, $D\gamma_0$ [where $1 = (Dr)^{1/2}$ is the diffusion length] are certainly satisfied; this allows us to neglect the term $v_0(\partial n/\partial z)$ in the first equation (24). Furthermore, we will assume that $\xi(x, t)$ changes little in a time $t \approx t_0 \approx \max\{1/D\gamma_0^2, 1^2/D, 1/Dg^2\}$. Then for $t >$ to a quasi-steady-state regime is established, which is equivalent to assuming that $\xi(x, t)$ and $\partial\xi(x, t)/\partial t$ do not depend on time. The steady-state solution to the problem (24), (25) we will seek in the form

$$n(x, z) = n_0(z) + [n_1(z)e^{-igx} + n_2(z)e^{-i2gx} + \text{c.c.}]. \quad (26)$$

In order to write down equations for n_0 , n_1 , and n_2 , it is necessary to include in (24) the rescattering caused by cross terms of the type $(\partial^2\xi/\partial x^2)(\partial n/\partial z)$, $(\partial\xi/\partial x)(\partial^2 n/\partial x\partial z)$, $(\partial\xi/\partial x)(\partial n/\partial x)$. Below we will see that $\partial n_0/\partial z = Af_0$, $\partial n_2/\partial z = Bf_{2g}$, $\partial n_1/\partial z = Cf_g$, where A , B , C are quantities of order one, while the amplitudes of the profile satisfy the conditions $g\xi_g \lesssim \beta_n^{1/2}$, $g\xi_{2g} < \beta_n^{1/2}$ ($\beta_n \ll 1$) for all values of t . For the grating with parameters (1), it follows from Eqs. (20)–(22) that when $g\xi_g \approx \beta_n^{1/2}$ the grating amplitudes are in the ratios

$$|f_0|_{\max} : |f_{2g}|_{\max} : |f_g|_{\max} = 1:1:\beta_n^{1/2}.$$

From the estimates which follow from this ratio it is quite clear that it is sufficient to include in (24) only the rescattering $n_0 \rightarrow n_1$ and $n_2 \rightarrow n_1$ by the grating g . The nonlinearities which arise because of rescattering we will refer to as "topological". As a result, after substituting (26), (4) into (24), (25) we obtain the following system determining $n_0(z)$:

$$D \frac{\partial^2 n_0}{\partial z^2} - \frac{n_0}{\tau} = -kf_0 e^{-\gamma_0 z}, \quad (27)$$

$$n_0(z=\infty) = 0, \quad \left. \frac{\partial n_0}{\partial z} \right|_{z=0} = \frac{SN}{D} v_0, \quad v_0 = \beta n_0(z=0).$$

The distribution $n_2(z)$ is the solution to the problem

$$D \left(\frac{\partial^2}{\partial z^2} - 4g^2 - \frac{1}{\tau} \right) n_2 = -kf_{2g} e^{-\gamma_0 z}, \quad n_2(z=\infty) = 0, \quad (28)$$

$$\left. \frac{\partial n_2}{\partial z} \right|_{z=0} = \frac{SN}{D} \frac{\partial \xi_{2g}}{\partial t}, \quad \frac{\partial \xi_{2g}}{\partial t} = \beta n_2(z=0),$$

while the concentration $n_1(z)$ is found from the system of equations

$$D \left(\frac{\partial^2}{\partial z^2} - g^2 - \frac{1}{\tau} \right) n_1 = -Dg^2 \xi_g \frac{\partial n_0}{\partial z} + 3Dg^2 \xi_g^* \frac{\partial n_2}{\partial z} - kf_g e^{-\gamma_0 z},$$

$$n_1(z=\infty) = 0, \quad \left(\frac{\partial n_1}{\partial z} - 2g^2 \xi_g^* n_2 \right)_{z=0} = \frac{SN}{D} \frac{\partial \xi_g}{\partial t}, \quad (29)$$

$$\frac{\partial \xi_g}{\partial t} = \beta n_1(z=0).$$

It is clear from (27)–(29) that the solutions to these problems must be found in the form

$$n_0(z) = A_0 \exp(-\gamma_0 z) + B_0 \exp(-\delta_0 z),$$

$$n_2(z) = A_2 \exp(-\gamma_0 z) + B_2 \exp(-\delta_2 z),$$

$$n_1(z) = C_1 \exp(-\gamma_0 z) + C_2 \exp(-\delta_1 z)$$

$$+ C_3 \exp(-\delta_0 z) + C_4 \exp(-\delta_2 z),$$

$$\delta_0 = 1/l, \quad \delta_1 = (g^2 + l^{-2})^{1/2}, \quad \delta_2 = (4g^2 + l^{-2})^{1/2},$$

where A_0 , B_0 , A_2 , B_2 , C_1, \dots, C_4 are constants. Substituting these solutions into (27)–(29) allows us to find equations which determine the time evolution of the fundamental and first harmonic of the surface profile, and also the spatially homogeneous etching rate $v_0(t)$:

$$\frac{\partial \xi_g}{\partial t} = \frac{\beta k}{(\delta_1 D + SN\beta)(\delta_1 + \gamma_0)} \times \left\{ f_g - f_0(g\xi_g) \frac{g(\gamma_0 \delta_0 D - \delta_1 SN\beta)}{(\delta_0 + \gamma_0)(\delta_0 + \delta_1)(\delta_0 D + SN\beta)} - f_{2g}(g\xi_g^*) g \frac{D[2\delta_1(\delta_1 + \delta_2) + (2\delta_1 - \delta_2)\gamma_0] + 3\delta_1 SN\beta}{(\delta_2 + \gamma_0)(\delta_2 + \delta_1)(\delta_2 D + SN\beta)} \right\},$$

$$\frac{\partial \xi_{2g}}{\partial t} = \frac{\beta}{(\delta_2 + SN\beta)} \frac{k f_{2g}}{(\gamma_0 + \delta_2)}, \quad v_0 = \frac{k \beta f_0}{(\delta_0 D + SN\beta)(\gamma_0 + \delta_0)}. \quad (30)$$

For the PCE process the conditions $SN\beta \ll D\delta_0$, $D\delta_1$, $D\delta_2$, and $D\gamma_0$ are certainly fulfilled. Taking this into account, we can investigate two limiting cases. For $lg \gg 1$ the time evolution of the surface profile is described, according to (30), by the equations

$$\frac{\partial \xi_g}{\partial t} = \frac{\beta k}{Dg(\gamma_0 + g)} \left\{ f_g - \frac{\gamma_0 l}{(\gamma_0 l + 1)} f_0(g\xi_g) - \frac{g}{(\gamma_0 + 2g)} f_{2g}(g\xi_g^*) \right\},$$

$$\frac{\partial \xi_{2g}}{\partial t} = \frac{\beta k}{2Dg(\gamma_0 + 2g)} f_{2g}, \quad v_0 = \frac{\beta k l^2}{D(\gamma_0 l + 1)} f_0. \quad (31)$$

For the regime $|g\xi_g| \approx \beta_n^{1/2}$ it is necessary to take into account the second and third terms in the curly brackets of (31), i.e., the topological nonlinearities due to rescattering of the concentration waves $n_0 \rightarrow n_1$ and $n_2 \rightarrow n_1$ by the grating g . This is because

$$|f_g| \approx f_0 \beta_n^{1/2} \approx |f_{2g}| \beta_n^{1/2}$$

for this case. In the other limiting case, for lg , $1\gamma_0 \ll 1$, from (30) we obtain

$$\frac{\partial \xi_g}{\partial t} = \frac{\beta k l^2}{D} f_g, \quad \frac{\partial \xi_{2g}}{\partial t} = \frac{\beta k l^2}{D} f_{2g}, \quad v_0 = \frac{\beta k l^2}{D} f_0. \quad (32)$$

Thus, the question of when these topological nonlinearities play a role in PCE can be answered based on the semiconductor parameters and the wavelength of the laser radiation.

b. The physics of profile generation in the case of LE is the same as for PCE, with the difference that the role of the concentration $n(x, z, t)$ is played by the temperature $T(x, z, t)$, while the velocity of the moving boundary between the media in the system of coordinates x, y, z is described by

the law

$$v_z(t) = v_0(t) + \partial \xi(x, t) / \partial t = C_0 \exp[-U/RT(x, z=0, t)], \quad (33)$$

where C_0 is a constant determined by the experimental data, $R = k_B N$, k_B is Boltzmann's constant, N is the number of atoms per unit volume, and U is the activation energy per unit volume. The problem of laser heating of the surface (4) can be described by (24), (33), if in (24) we make the replacement

$$n \rightarrow T - T_I, D \rightarrow \chi, \tau \rightarrow \infty, k \rightarrow 1/C_p, SN/D \rightarrow L/\kappa, \quad (34)$$

where T_I is the initial temperature of the surface, χ is the coefficient of thermal conductivity, and $\kappa = \chi C_p$; C_p, L are the heat capacity and latent heat of evaporation per unit volume. The solution to (24), (33), (34) will be sought in the form

$$T(x, z, t) = T_0(z, t) + [T_1(z, t)e^{-ix} + T_2(z, t)e^{-iz} + \text{c.c.}].$$

Because $T \gg |T_1|, |T_2|$, after linearizing (33) we obtain in place of (25)

$$v_0 = C_0 \exp(-U/RT_{0n}), \quad \frac{\partial \xi_g}{\partial t} = \frac{Uv_0}{RT_{0n}^2} T_1(z=0, t), \quad (35)$$

$$\frac{\partial \xi_{2g}}{\partial t} = \frac{Uv_0}{RT_{0n}^2} T_2(z=0, t),$$

where $T_{0n} = T_0(z=0, t)$. Making the same sort of approximations as those discussed after Eq. (26), the distribution $T_0(z, t)$ is given not by (27) but by the system

$$\frac{\partial T_0}{\partial t} - v_0 \frac{\partial T_0}{\partial z} = \chi \frac{\partial^2 T_0}{\partial z^2} + \frac{1}{C_p} f_0 e^{-\gamma_0 z},$$

$$T_0(z, t=0) = T_0(z=\infty, t) = T_I, \quad (36)$$

$$T_0(z=0, t) = T_{0n}, \quad \left. \frac{\partial T_0}{\partial z} \right|_{z=0} = \frac{L}{\kappa} v_0,$$

$$v_0 = C_0 \exp(-U/RT_{0n}),$$

when the conditions $v_0 \ll \chi g, \chi \gamma_0$ and $t_0 \approx 1/\chi g^2, 1/\chi \gamma_0^2$ are fulfilled, the distributions $T_1(z, t), T_2(z, t)$ are determined by the quasistationary problems which follow from (28), (29) with the help of the substitution (34) and the substitution

$$\beta \rightarrow Uv_0/RT_{0n}^2. \quad (37)$$

[see (25), (26), (27)].

The stationary solution to the problem (26) applies for $t \gtrsim \chi/v_0^2$. For LE the characteristic values are $v_0 \approx 5 \cdot 10^2$ cm/sec and $\chi \approx 0.1$ cm²/sec. This implies that for the LE process, in contrast to PCE, both the stationary ($t \gtrsim 10^{-6}$ sec) and nonstationary ($t \lesssim 10^{-6}$ sec) regimes can be realized in practice. For the stationary case the solution to the system (36) ($t \gtrsim \chi/v_0^2$) has the form

$$T_0(z) = T_n + A_0 e^{-\gamma_0 z} + B_0 e^{-v_0 z/\chi}, \quad (38)$$

$$A_0 = -\frac{f_0}{\kappa \gamma_0^2}, \quad B_0 = \frac{f_0}{\gamma_0 v_0 C_p} - \frac{L}{C_p},$$

in this case v_0 and t_{0n} are determined from the transcendental equations³⁶

$$v_0 = f_0/\gamma_0 [L + C_p(T_{0n} - T_I)], \quad v_0 = C_0 \exp(-U/RT_{0n}). \quad (39)$$

In the nonstationary regime ($t \lesssim \chi/v_0^2$), when the conditions $z^2 \ll 4\chi t, t \gtrsim 1/\chi \gamma_0^2, v_0 \ll \chi \gamma_0$ are fulfilled, the solution to (36) can be cast in the form

$$T_0(z, t) \approx (2f_0/\gamma_0 C_p - 2Lv_0/C_p) \left(\frac{t}{\pi \chi}\right)^{1/2} - \frac{f_0}{\chi \gamma_0^2} (e^{-\gamma_0 z} + \gamma_0 z) + \frac{Lv_0 z}{\kappa} + T_I. \quad (40)$$

In deriving the dynamic equations for v_0, ξ_g, ξ_{2g} , we should substitute in the system (29), (34), and (37) either the solutions (28), (34), (37), and (38), (39) for the stationary regime, or the solutions (28), (34), (37), and (40) for the nonstationary regime. It turns out that when the inequalities $v_0 \ll \chi g, \chi \gamma_0$, and $t \gtrsim \chi g^2, \chi \gamma_0^2$ are fulfilled, for both regimes the time evolution of the fundamental and first harmonic of the surface profile is described by the equations

$$\frac{\partial \xi_g}{\partial t} = \frac{(\gamma_0 + g)^{-1}}{L + g\kappa RT_{0n}^2/Uv_0} \left\{ f_g - f_0(g\xi_g) + (\gamma_0 + g)Lv_0(g\xi_g) - \frac{g}{\gamma_0 + 2g} f_{2g}(g\xi_g^*) \right\}, \quad (41)$$

$$\frac{\partial \xi_{2g}}{\partial t} = \frac{1}{[L + 2g\kappa RT_{0n}^2/Uv_0] (\gamma_0 + 2g)} f_{2g},$$

In the stationary case v_0 and T_{0n} are determined by Eq. (39), while in the nonstationary regime they are given, according to (40), by the expressions

$$v_0 = C_0 \exp(-U/RT_{0n}), \quad T_{0n} \approx (2f_0/\gamma_0 C_p - 2Lv_0/C_p) (t/\pi \chi)^{1/2}. \quad (42)$$

The second and third terms in curly brackets of the first equation of (41) are due to the rescattering $T_0 \rightarrow T_1$ by the grating g , while the fourth term is due to the similar rescattering $T_2 \rightarrow T_1$. Note that in the regime where (39) applies, the values of T_{0n} and v_0 are larger than in the regime (42).

Let us now clarify the conditions under which we must include the topological nonlinearities in (41). Let us first investigate the stationary case (39). After substituting (39) into (41), we find that

$$\frac{\partial \xi_g}{\partial t} = [(\gamma_0 + g)(L + g\kappa RT_{0n}^2/Uv_0)]^{-1} \times \{ f_g - \alpha f_0(g\xi_g) - \nu f_{2g}(g\xi_g^*) \},$$

$$\frac{\partial \xi_{2g}}{\partial t} = [(\gamma_0 + 2g)(L + 2g\kappa RT_{0n}^2/Uv_0)]^{-1} f_{2g}, \quad (43)$$

where

$$\alpha = [\gamma_0 C_p(T_{0n} - T_I) - gL]/\gamma_0 [L + C_p(T_{0n} - T_I)], \quad \nu = g/(\gamma_0 + 2g). \quad (44)$$

In the regime where (39) holds, numerical calculations show that for quartz, mercury, and germanium, and characteristic experimental intensities $I_1 = 2$ to $5 \cdot 10^7$ W/cm², the second and third terms in the curly brackets in (41) balance each other; this allows the coefficient α in (44) to take on the values 0.1 to 0.4, depending on the intensity and material parameters, while $\nu = 0$ to 0.5. In these cases, when $\alpha \approx \nu \approx 0$ and $L \gg g\kappa RT_{on}^2 / Uv_0$, Eq. (43) acquires a simpler form analogous to the form of Eq. (32) for PCE:

$$\partial \xi_{gs} / \partial t = f_{gs} / \gamma_0 L, \quad \partial \xi_{2s} / \partial t = f_{2s} / \gamma_0 L.$$

For real experimental conditions the inequality $L \gg g\kappa RT_{on}^2 / Uv_0$ is equivalent to the condition $\lambda \gg 0.1$ to 2 microns; for the optical range these inequalities should be verified in each specific case.

In experiments on the formation of structures under pulsed conditions, the pulse length is usually $\tau_p = 20$ to 200 nsec; consequently the nonstationary regime (42) is in effect. Since v_0 and T_{on} given by (42) are much smaller than v_0 and T_{on} given by (39), according to (41) the evolution equations for the profile in regime (42) have the form (43), where

$$\alpha = 1, \quad \nu = g / (\gamma_0 + 2g).$$

Thus, in the nonstationary case the topological nonlinearities always play an important role in an investigation of the evolution of the profile up to the level $|g\xi_{gs}| \approx \beta_n^{1/2}$.

In Refs. 29, 34, 35, where the profile evolution was studied only up to the level $|g\xi_{gs}| \approx \beta_n$, the neglect of the topological nonlinearities is permissible. We will discuss the region of validity of this paper below. However, in Refs. 31, 33, the topological nonlinearities were not included, although there the profile dynamics were investigated up to the level $|g\xi_{gs}| \approx \beta_n^{1/2}$. Therefore the results of Refs. 31, 33 must be regarded as qualitative. Let us note that in contrast to the conclusions of Ref. 33, it is easy to see from Eqs. (41) and (43), taking (20)–(22) into account, that in both the stationary and nonstationary regimes there is no intensity threshold within the LE model for the generation of a surface profile. Therefore the results for generation of a profile slightly above threshold which were obtained in Ref. 33 appear to us to be invalid.

4. OSCILLATORY REGIME FOR GENERATION OF FIRST AND SECOND HARMONICS OF A PROFILE: REFLECTIVITY AND ABSORPTIVITY OF A SURFACE DURING LE AND PCE

Let us substitute Eqs. (20)–(23) into Eqs. (32), (43), assuming in (43) that $L \gg g\kappa RT_{on}^2 / Uv_0$. So as to represent these equations in a convenient form, let us introduce a normalized time and a normalized phase and amplitude of the surface gratings:

$$\tau = 2\gamma_L t, \quad \xi_{ng} = \xi_n \exp(-i\varphi_n),$$

$$n = 1, 2, 3; \quad \Phi_1 = 2\varphi_1 - \varphi_2, \quad \Phi_2 = \varphi_1 + \varphi_2,$$

$$x_1 = g\xi_1 / \beta_n, \quad x_2 = 2g^2\xi_2 / k_0 \varepsilon_0^{1/2} \beta_n, \quad x_3 = g\xi_3 / \beta_n,$$

where the quantity γ_L equals

$$\begin{aligned} \gamma_L = \gamma_{LE} &\equiv \frac{1}{L\gamma_0} \frac{2\omega \varepsilon'' k_z^2}{\pi |\gamma|^2} \frac{g^2}{k_0 \varepsilon_0^{1/2} \beta_n} |E_{ix}|^2, \\ \gamma_L = \gamma_{PCE} &\equiv \frac{\beta k l^2}{D} \frac{2\omega \varepsilon'' k_z^2}{\pi |\gamma|^2} \frac{g^2}{k_0 \varepsilon_0^{1/2} \beta_n} |E_{ix}|^2 \end{aligned} \quad (45)$$

for LE and PCE respectively. We recall that E_i is the electric field intensity in the medium with dielectric permittivity ε_0 ; $\varepsilon_0 = 1$ for LE and $\varepsilon_0 \neq 1$ for PCE, and $\gamma_0 \approx 2mk_0$. Since what interests us is the evolution of gratings with the parameters (1), for which $k_g^2 = k_i^2 + g^2 \approx k_0^2 \varepsilon_0$, we set $g \approx k_z = k_0 \varepsilon_0^{1/2} \cos \theta$, $\Gamma_{2g} \approx 3^{1/2} k_0 \varepsilon_0^{1/2} \cos \theta$, $\Gamma_{3g} \approx 8^{1/2} k_0 \varepsilon_0^{1/2} \cos \theta$. As a result, in the region $k_g^2 > k_0^2 \varepsilon_0$ the system which describes the generation of the fundamental and first harmonic of the profile can be written in the form

$$\begin{aligned} \frac{dx_1}{d\tau} &= \frac{x_1}{\Delta_0^2} \left\{ A(1+A^2-x_2^2) + (A^2-1-x_2^2)x_2 \cos \Phi_1 \right. \\ &\quad \left. - \frac{1 + \sin^2 \theta + 3^{3/2} \alpha}{3^{3/2} \cos \theta} \beta_n [(1+A^2)x_1^2 + x_1^2 x_2^2 + 2x_1^2 x_2 A \cos \Phi_1] \right. \\ &\quad \left. - \alpha \beta_n \frac{(A^2+1)^2 - 2x_2^2(A^2-1) + x_2^4}{2 \cos \theta} \right. \\ &\quad \left. - \nu \beta_n \frac{\cos 2\theta}{2 \cos \theta} [(1+A^2)x_1^2 + x_1^2 x_2^2 \cos 2\Phi_1 \right. \\ &\quad \left. + 2x_1^2 x_2 A \cos \Phi_1] \right\} + F_1 x_2 x_3 \cos(\Phi_2 - \varphi_3), \end{aligned} \quad (46)$$

$$\begin{aligned} \frac{dx_2}{d\tau} &= \frac{x_1^2 \cos 2\theta}{\Delta_0^2} \{ 2Ax_2 + (A^2+1+x_2^2) \cos \Phi_1 \} \\ &\quad + F_2 x_1 x_3 \cos(\Phi_2 - \varphi_3), \\ \frac{d\Phi_1}{d\tau} &= \frac{1}{\Delta_0^2} \left\{ 2(1-A^2+x_2^2)x_2 - \frac{x_1^2 \cos 2\theta}{x_2} (A^2+1-x_2^2) \right\} \sin \Phi_1 \\ &\quad + (2F_1 x_2 x_3 / x_1 - F_2 x_1 x_3 / x_2) \sin(\Phi_2 - \varphi_3), \\ \frac{d\Phi_2}{d\tau} &= \frac{1}{\Delta_0^2} \left\{ (1-A^2+x_2^2)x_2 + \frac{x_1^2 \cos 2\theta}{x_2} (A^2+1-x_2^2) \right\} \sin \Phi_1 \\ &\quad + (F_1 x_2 x_3 / x_1 + F_2 x_1 x_3 / x_2) \sin(\Phi_2 - \varphi_3). \end{aligned}$$

Here, x_3 and φ_3 are assumed to be time-independent and Δ_0^2 is the renormalized squared modulus of the resonant denominator (11). The quantity A takes into account anharmonicity in the dispersion law (7), while the coefficients F_1 , F_2 characterize the diffraction "seeds" (23). These quantities are given by the following expressions

$$\begin{aligned} \Delta_0^2 &= (1-A^2+x_2^2+2\beta_n x_1^2 \cos \theta)^2 \\ &\quad + 4(A+A\beta_n x_1^2 \cos \theta + \beta_n x_1^2 x_2 \cos \theta \cos \Phi_1)^2, \\ A &= B - \frac{\beta_n \cos \theta}{3^{1/2}} x_1^2 - \frac{\beta_n}{8^{1/2} \cos \theta} x_2^2, \\ B &= \frac{1}{\beta_n} \left[\frac{(k_g^2 - k_0^2 \varepsilon_0)^{1/2}}{k_0 \varepsilon_0^{1/2}} - \beta_m \right], \end{aligned} \quad (47)$$

$$\begin{aligned} F_1 &= \frac{\beta_n^2}{2 \cos^2 \theta} \left(1 + \frac{1+5 \sin^2 \theta}{\sqrt{24} \cos^2 \theta} \right), \\ F_2 &= 2\beta_n^2 \left\{ \frac{1+2 \sin^2 \theta}{\beta_n} \left(\frac{A}{8^{1/2} \cos \theta} + 2\beta_n x_1^2 \right) + 1 \right\} \\ &\quad \times \frac{1}{1+A^2+4 \cos \theta x_1^2 (1 + \cos \theta \beta_n x_1^2) \beta_n}. \end{aligned}$$

The expression in square brackets in the first term of Eq. (8) for $\alpha = \nu = 0$ is due to the reactive nonlinearity, while the terms proportional to α and ν are due to the topological nonlinearities. The terms connected with the topological nonlinearities can be larger, e.g., for $\alpha = 1$, than those due to the reactive nonlinearity. It follows from (46), (47) that for $x_2 \gtrsim 1$ it is also important to include the terms caused by the intermode nonlinearity which are proportional to x_2 , whereas inclusion of the reactive and topological nonlinearities turns out to be necessary for $x_1 \gtrsim 1/\beta_n^{1/2}$.

The coefficient of specular reflection $R = |E_{0x}|^2/|E_{ix}|^2$ (and the absorptivity $1 - R$ for the surface (4) can be represented by using Eq. (9) in the form ($k_g^2 > k_0^2 \epsilon_0$)

$$R_n = \frac{R}{R_\phi} = \frac{1}{\Delta_0^2} \{ (1 - A^2 + x_2^2 - 2\beta_n x_1^2 \cos \theta)^2 + 4(A - A\beta_n x_1^2 \cos \theta - \beta_n x_1^2 x_2 \cos \theta \cos \Phi_1)^2 \}, \quad (48)$$

where $R_\phi = |k_z - i\gamma|^2/|k_z + i\gamma|^2$ is the Fresnel coefficient of specular reflection, and $\gamma = (k_t^2 - k_0^2 \epsilon)^{1/2} \approx (m - in)k_0$.

In the initial linear stages of the profile development, i.e., when $x_1 \gg 1/\beta_n^{1/2}$, $x_2 \ll 1$, if we neglect the "seeds", Eq. (46) can be written in the form

$$\frac{dx_1}{d\tau} = \frac{B}{1+B^2} x_1, \quad \frac{dx_2}{d\tau} = \frac{\cos 2\theta \cos \Phi_1}{1+B^2} x_1^2, \quad (49)$$

$$\frac{d\Phi_1}{d\tau} = -\frac{x_1^2 \cos 2\theta}{x_2(1+B^2)} \sin \Phi_1.$$

An analysis of (49) shows that when $2\theta < 90^\circ$ the structure with the most rapid growth in time is the one which corresponds to $A = B = 1$, i.e., a grating with parameters (1) and its first harmonic, for which $\Phi = 0$ (phase locking). In this case, if the seed amplitudes $x_{10} \neq 0$ and $x_{20} = 0$, then $x_1 = x_{10} \exp(\gamma_L t)$, $x_2 = (x_{10}^2 |\cos 2\theta|) [\exp(2\gamma_L t) - 1]/2$. At this stage x_2 grows more rapidly than x_1 , and has practically no effect on the evolution of the fundamental. The expressions for γ_L coincide with those obtained earlier in Refs. 37, 13, and are understood to be growth rates for the structures. For $2\theta > 90^\circ$ the equations for x_1 and x_2 remain the same; however, the phases are locked so that $\Phi_1 = \pi$.

In order to describe the subsequent stages, for which $x_1 \ll 1/\beta_n^{1/2}$, $x_2 \ll 1/\beta_n^{1/2}$, it is sufficient to include in Eqs. (46), (47) only the intermode nonlinearity. Then setting $A = B = 1$, $F_1 = F_2 = 0$, $\beta_n = 0$, we obtain

$$\begin{aligned} \frac{dx_1}{d\tau} &= \frac{x_1}{x_2^4 + 4} (2 - x_2^2 - x_2^3 \cos \Phi_1), \\ \frac{dx_2}{d\tau} &= \frac{x_1^2 \cos 2\theta}{x_2^4 + 4} [2x_2 + (2 + x_2^2) \cos \Phi_1], \\ \frac{d\Phi_1}{d\tau} &= \frac{\sin \Phi_1}{x_2^4 + 4} \left[2x_2^3 - \frac{x_1^2 \cos 2\theta}{x_2} (2 - x_2^2) \right]. \end{aligned} \quad (50)$$

The system (50) coincides with the system presented in Ref. 34. Finally, for $x_1 \approx 1/\beta_n^{1/2}$, $x_2 > 1$, it is necessary to use the system (46), (47).

Below we will illustrate the role of all the nonlinearities described above with specific examples. Let us first investi-

gate the process of evaporation of a metallized alloy of germanium under the action of radiation from a neodymium laser ($\lambda = 1.06 \mu$, $\epsilon = -32 + i72$ (Ref. 38), $\epsilon_0 = 1$). In this case we have $\beta_n = 0.06$, $\beta_m = 0.094$. We will assume that the initial amplitudes $\xi_{10} = \xi_{20} = \xi_{30} \approx 25 \text{ \AA}$. Because we are interested in the evolution of the grating (1) and its first harmonic, we set $B = 1$ in (47).

To begin with let us clarify the region of applicability of Eq. (50). In the theory (Ref. 34) these equations are investigated analytically using the separatrix approximation, assuming that in the generation process the phase Φ_1 changes discontinuously, alternating between the two values $\Phi_1 = 0$ and $\Phi_1 = \pi$. In this approximation it follows from (50) that for $2\theta < 90^\circ$ the time evolution of the profile takes place in the form of opposite-phase oscillations of x_1 and x_2 ; the n th maximum $(x_2)_{\max}^{(n)} \approx 2n$, while the n th maximum $(x_1)_{\max}^{(n)} \approx (2n - 1)/\cos^{1/2} 2\theta$. These expressions are confirmed by Fig. 2, where the results of a numerical solution of (50) are shown. It is clear from Fig. 2, however, that the variation of Φ_1 from 0 to π takes place quite smoothly; therefore the expressions for $(x_1)_{\max}^{(n)}$ and $(x_2)_{\max}^{(n)}$ are obeyed only approximately. As the amplitude grows the "period" of the oscillations increases.

In Fig. 3 we present plots of the time evolution of the profile and the normalized coefficient of specular reflection (48). These plots are based on the numerical solution of (46), (47), taking into account all the nonlinearities, with the exception of the topological ones (i.e., $\alpha = \nu = 0$). It follows from Fig. 3 that after several oscillations of x_1 and x_2 the system arrives at a steady state oscillatory regime with bounded values of the amplitudes. In this case the coefficient of specular reflection undergoes high-amplitude oscillations which periodically result in its total suppression and 100% absorption of the radiation by the surface at specific instants of time. When we neglect the reactive nonlinearity the amplitude x_1 saturates at the point where the second term in (47) for A is comparable to unity, whereas when the reactive nonlinearity is taken into account it occurs at the point where the first term in square brackets of the first equation in (46) (for $x_2 \approx 0$) balances the first term in curly brackets of

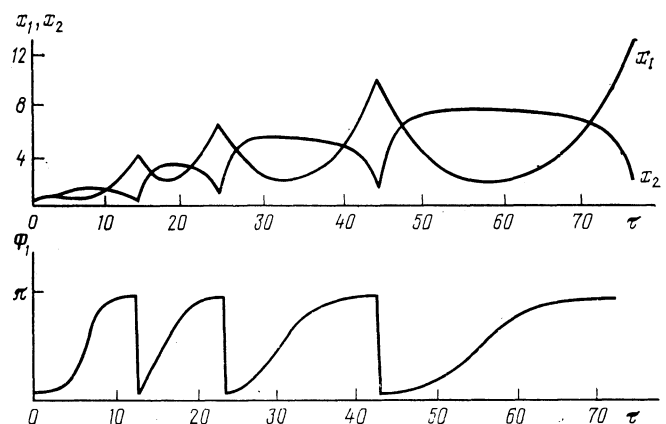


FIG. 2. Time evolution of x_1 , x_2 and Φ_1 during LE of germanium. The plots were constructed using numerical solution of the system (46), (47) for $\beta_n = 0$, $\theta = 35^\circ$, $A = B = 1$, $F_1 = F_2 = 1$, or, which is the same thing, numerical solution of the system (50).

this equation. When we use the separatrix approximation in (46), (47), it is easy to obtain a rough estimate of the number of oscillations n_c which precede the steady-state regime in these two cases; thus,

$$n_c \approx \left(\frac{3^{1/2} \cos 2\theta}{4\beta_n \cos \theta} \right)^{1/2} + 0.5 \approx 2.24;$$

$$n_c \approx \left(\frac{3^{1/2} \cos \theta \cos 2\theta}{4\beta_n (1 + \sin^2 \theta)} \right)^{1/2} + 0.5 \approx 1.7.$$

Therefore, in the region of optical wavelengths the theory of Ref. 34 gives a valid qualitative description of the dynamics of x_1 and x_2 only for the first two or three oscillations. This conclusion is also verified by comparing Figs. 2 and 3. As for the results of Ref. 35, in our opinion the amplitudes of the diffracted fields in the medium were calculated incorrectly. Therefore the region of applicability of the theory in Ref. 35 is limited to the linear stages of the development of SPS.

Plots based on the same parameters as in Fig. 3, but with the values $F_1 = F_2 = 0$, show that with each oscillation the minimum value of the amplitude of x_1 approaches closer and closer to zero. Therefore more and more time is required to depart from this minimum, leading to an increase in the period of oscillations with time. The introduction of diffractive seeds $F_1 \neq 0$ and $F_2 \neq 0$ into the system (46) prevents the approach of x_1 to zero and thus stabilizes the period of oscillations of the fundamental and first harmonic of the profile. The second function brings about the diffractive "seeding" in the following way. If at the initial time we have $\Phi_1 = \Phi_{10} = 0$ (which corresponds to the most rapidly-growing grating x_2), then in the absence of diffractive seeds $\Phi_1 = 0$ holds for all time. In this case the oscillatory regime does not arise.²⁹ If, however, we have $0 < \Phi_{10} < \pi$, then the oscillatory regime is established, and $0 < \Phi_1 < \pi$ holds for all

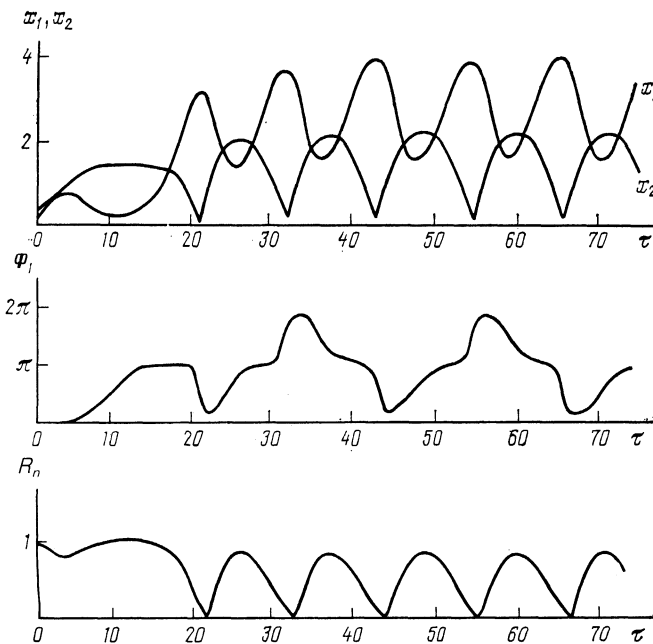


FIG. 3. Time evolution of x_1 , x_2 , Φ_1 and R_n during LE of germanium. The plots were constructed through numerical solution of Eqs. (46), (47) for $\beta_n = 0.06$, $\theta = 35^\circ$, $B = 1$, $F_1 \neq 0$, $F_2 \neq 0$, $\varphi_3 = 1$ rad, $\alpha = \nu = 0$.

τ (see Fig. 2). When the diffractive seeds are included the oscillatory regime arises for any Φ_{10} ; in this case the phase can be "expelled" from the phase-locking points $\Phi_1 = 0$ or $\Phi_1 = \pi$ both in the region $0 < \Phi_1 < \pi$ and in the regions $\Phi_1 < 0$ and $\Phi_1 > \pi$. The variation in the phase φ_3 does not affect the character of the steady-state oscillations.

Let us clarify why the oscillatory regime was not predicted by Ref. 31, in which this very problem was solved numerically for all epochs using the same parameters (except that $\theta = 0^\circ$). It is easy to see from Eqs. (46), (47), and from the solution (49), that on the time scale τ the position of the first maximum and subsequent minimum of x_1 (see Fig. 3) depends only weakly on θ . Therefore the positions of the first minima for $\theta = 0^\circ$ and $\theta = 35^\circ$ must practically coincide. In Ref. 31 the numerical calculation was carried out up to the normalized time $\tilde{t} = k_0 I_i t / 2\pi L = 0.25$. In our normalized units (45) for $\theta = 0^\circ$ the instant $t = 0.25$ must correspond in Fig. 3 to the instant $\tau = 8k_0 I_i t / L = 16\pi\tilde{t} = 12.5$. From Fig. 3 it is clear that for $\tau = 12.5$ the amplitude x_1 is close to zero, while the value x_2 is maximal, and in the neighborhood of $\tau = 12.5$ the amplitudes x_1 , x_2 change very slowly. Therefore there is quantitative agreement between our results and those of Ref. 31 in the region $0 \leq \tau \leq 12.5$ holds (see Fig. 3 and curve 1 of Fig. 4 in Ref. 31). The absence of any conclusions in Ref. 31 concerning the oscillatory character of the profile formation process is connected, in our opinion, with the smallness of the time interval over which the numerical solution was carried out ($0 \leq \tilde{t} \leq 0.25$).

From Eqs. (46), (47) it follows that for angles $\theta > 45^\circ$ the generation must undergo an essential change. The numerical calculation shows that, irrespective of its initial value dependence, the phase Φ_1 becomes locked at $\Phi_1 = \pi$ after a time. In this case the amplitude x_1 grows approximately linearly with time up to the limit of applicability of the theory ($|\xi_g| < 1$), while the amplitude x_2 attains its stationary value.

Up until now we have assumed that a rectangular laser pulse acts at the surface. In Fig. 4 we show the effect of

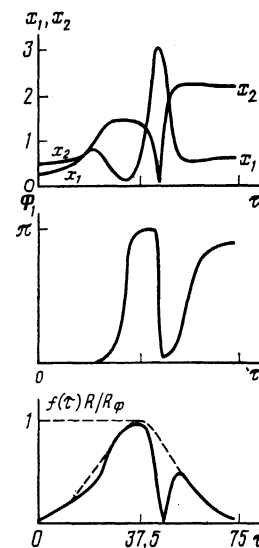


FIG. 4. Time evolution of x_1 , x_2 , Φ_1 , and the normalized specular reflection of the signal $f(\tau)R/R_\phi$, during evaporation induced by a laser pulse with a Gaussian temporal profile. In Eqs. (46)–(48) we set $\beta_n = 0.06$, $\theta = 35^\circ$, $B = 1$, $F_1 \neq 0$, $F_2 \neq 0$, $\varphi_3 = 1$ rad, $\alpha = \nu = 0$.

harmonic generation on the profile when the incident radiation has a Gaussian form in time

$$|E_{iz}|^2 = |E_{i0}|^2 f(\tau) = |E_{i0}|^2 \exp[-(\tau-37)^2/250].$$

From Fig. 4 it is clear that in the initial stage the specular reflection is practically the same as that from a plane surface, and then drops to zero; ultimately the pulse is reestablished at its initial level, although the resulting form of the profile is far from planar (see Fig. 4). This temporal behavior of the specular reflection, which is caused by the nonlinear generation of the surface profile, could serve as an explanation of the results of the experiments in Refs. 25–28 which were designed to investigate a considerable variation in the absorptivity and reflectivity of the surface observed under the action of a powerful laser pulse. It should be noted that the dependence of R_n on τ presented in Fig. 4 reproduces with extraordinary precision the experimentally measured dependence in Ref. 27 (see Fig. 5).

Let us now discuss the role of the topological nonlinearities during LE, setting $\alpha = 1$ and $\nu = 0$ (i.e., a metal in which $\gamma_0 \gg g$). It follows from a comparison of Figs. 3 and 6 that inclusion of topological nonlinearities leads to a significant decrease in the maximum values of x_1 and x_2 . In this case, total suppression of specular reflection does not occur, because for all τ the depth of the surface profile is less than optimum.⁶ Therefore, the feasibility of attaining 100% absorptivity hinges on whether or not we can neglect the topological nonlinearities (see Sec. 3).

Let us now investigate the PCE process in semiconductors. Assume *s*-polarized laser radiation with $\lambda = 0.53 \mu$ acts on the surface of the semiconductor *n*-GaAs which is submerged in the polishing etchant $H_2SO_4 : H_2O_2 : H_2O$ (Ref. 12). Then $n = 4.2$, $m = 0.33$ (Ref. 39), $\epsilon_0^{1/2} = 1.35$ (Ref. 12) and $\beta_n = 0.3$, $\beta_m = 0.025$. In Fig. 7 we show plots which illustrate the process of harmonic generation for this case in the regime where the topological nonlinearities are not required [see (32)]. In comparison with the case of LE of metallized germanium (compare with Fig. 3) the approach to the steady-state oscillatory regime occurs faster for PCE, while a deep dip in the specular reflection is observed even at the time of the first oscillation of x_1 . Let us estimate the real time required for one oscillation. Accord-

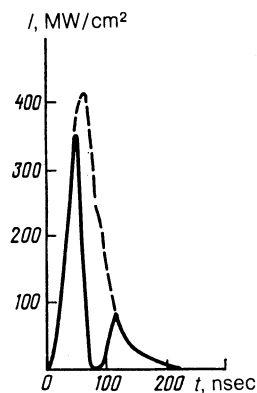


FIG. 5. Experimental dependence²⁷ of the intensity of incident (dashed curve) and specularly reflected (solid curve) signals for Al with $\theta = 10^\circ$ and $\lambda = 10.6 \mu$.

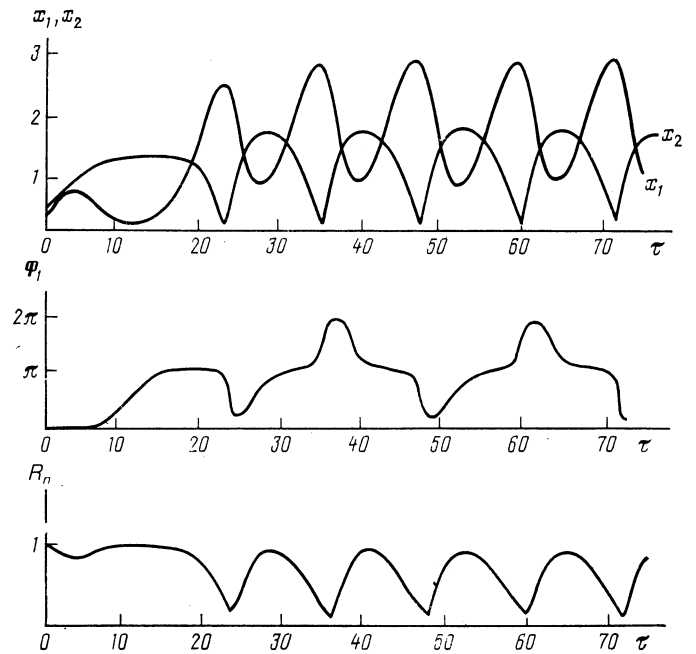


FIG. 6. Time evolution of x_1 , x_2 , Φ , and R_n taking into account the topological nonlinearities ($T_0 \rightarrow T_1$) during LE of germanium. The plots were constructed using numerical solution of Eqs. (46)–(48) for $\beta_n = 0.06$, $\theta = 35^\circ$, $B = 1$, $F_1 \neq 0$, $F_2 \neq 0$, $\varphi = 1$ rad, $\alpha = 1$, $\nu = 0$.

ing to Ref. 13, for our parameters the growth rate (45) for $I_i = 7 \text{ W/cm}^2$ and $\theta = 0^\circ$ equals $1/\gamma_L = 1.4 \text{ sec}^{-1}$. Then scaling according to Eq. (45) for $I_i = 1 \text{ W/cm}^2$ and $\theta = 35^\circ$ gives $1/\gamma_L = 11 \text{ sec}^{-1}$. Because $t = \tau/2\gamma_L$ and the average normalized time of one oscillation is $\tau = 22$ (see Fig. 7), for $I_i = 1 \text{ W/cm}^2$ we should expect a repetition of the oscillations during the time interval $t = 2$ min. This implies that in order to observe the oscillatory character of the generation of surface harmonics during PCE it is necessary to use a CW laser.

5. CONCLUSION

Besides the LE and PCE processes, we have also investigated the processes of pyrolytic etching and deposition.⁴⁰ In these processes, for all cases realized in practice it is necessary to include the topological nonlinearities in order to describe the nonlinear regime of SPS generation up to a level $g\epsilon_g \approx \beta_n^{1/2}$. The characteristic dependence of x_1 , x_2 , and R_n on τ is analogous to that shown in Fig. 6, with the sole difference that these quantities vary more abruptly with time in the region of the dip in $R_n(\tau)$.

The theory proposed here can serve as a basis for development of a single-step maskless technology for preparation of deep harmonic and biharmonic diffraction gratings with various reflective properties. In this case the depth of the profile and the ratio between the amplitudes of the fundamental and first harmonic are controlled by the exposure time, while the area of the grating can be increased by scanning the incident beam along the surface.^{17,22,41} It is significant that the period of the generated grating can be up to $2\epsilon_0^{1/2} n^*$ times smaller than the wavelength λ of the incident radiation.

With regard to experiment, the nonlinear regime for generation of surface structures has been little investigated.

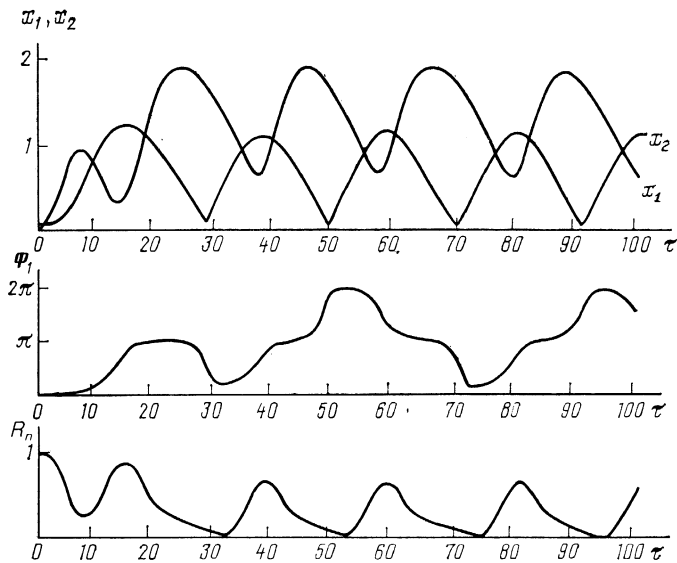


FIG. 7. Time evolution of x_1 , x_2 , Φ_1 , and R_n during PCE of n -GaAs. The plots were constructed through numerical solution of Eqs. (46)–(48) for $\beta_n = 0.3$, $\theta = 35^\circ$, $B = 1$, $F_1 \neq 0$, $F_2 \neq 0$, $\varphi = 1$ rad, $\alpha = \nu = 0$.

In this connection we note that the PCE process may turn out to be a good candidate for verifying this theory experimentally. First of all, in contrast to the processes of LE or generation of capillary waves,^{7,10} we do not require the inclusion of any nonlinearities (e.g., thermal, hydrodynamic, etc.) other than electrodynamic for its description. Secondly, the PCE process is not complicated by competition between the processes which lead to generation of surface profiles, e.g., thermocapillary forces or forces due to recoil of vapors during evaporation.^{7–10} And, finally, the slow evolution of the Fourier harmonic profile (seconds to tens of minutes) suggests the experimental possibility of continuous monitoring of the structures using simple apparatus.

In constructing a theory we have used the so-called discrete-mode approximation,²⁹ in which out of the entire continuum of induced gratings we consider only the dominant SPS. An estimate of the time interval for which the discrete-mode model is valid can be given only after the solution of a more complicated problem, where we include the effect of all the remaining spectrum of generated structures on the evolution of the profile.

The authors express their gratitude to S. A. Akhmanov, B. Ya. Panchenko and V. V. Kapaev for useful discussions of the results of the work, and also to V. M. Shabunin for his assistance in carrying out the numerical calculations.

¹ *Giant Raman Scattering*, R. Chenga and T. Futaka eds., Mir, Moscow, 1984.

² V. I. Emil'yanov and N. I. Koroteev, *Usp. Fiz. Nauk* **135**, 345 (1981) [*Sov. Phys. Usp.* **24**, 864 (1981)].

³ D. Maystre and R. Petit, *Opt. Commun.* **17**, 196 (1976); M. Hutley and D. Maystre, *Opt. Commun.* **19**, 431 (1976).

⁴ G. M. Gandel'man and P. S. Kondrateko, *Pis'ma Zh. Eksp. Teor. Fiz.* **38**, 246 (1983) [*JETP Lett.* **38**, 291 (1983)]; V. I. Konov and V. N. Tokarev, Preprint **70**, Ioffe Institute of Physics, USSR Acad. Sci., Moscow, 1985.

⁵ V. I. Emil'yanov, V. N. Semigonov, and V. I. Sokolov, *Kvant. Elektron.* (Moscow) **14**, 33 (1987) [*Sov. J. Quantum Electron.* **17**, 17 (1987)]; V. I. Emil'yanov and V. N. Semigonov, *Kvant. Elektron.* (Moscow) **14**, 47 (1987) [*Sov. J. Quantum Electron.* **17**, 26 (1987)].

⁶ S. A. Akhmanov, V. N. Semigonov, and V. I. Sokolov, *Zh. Eksp. Teor. Fiz.* **93**, 1654 (1987) [*Sov. Phys. JETP* **66**, 945 (1987)]; S. A. Akhmanov, S. V. Alekseev, V. N. Semigonov, and V. I. Sokolov, Preprint **26**, Center for Sci. Res. on Laser Tech., USSR Acad. Sci., Troisk, 1987.

⁷ S. A. Akhmanov, N. I. Koroteev, V. I. Emil'yanov, and V. N. Semi-

gonov, *Usp. Fiz. Nauk* **147**, 675 (1985) [*Sov. Phys. Usp.* **28**, 864 (1985)].

⁸ H. M. Van Driel, J. E. Sipe, and J. F. Young, *J. Lumin.* **30**, 446 (1985).

⁹ A. E. Siegman and P. M. Fauchet, *IEEE J. Quantum Electron.* **QE-22**, 1384 (1986).

¹⁰ V. I. Emil'yanov and V. N. Semigonov, *Science and Technology Summaries: Series on the Principles of Laser and Beam Technology*, VINITI, Moscow, **1**, 118 (1988).

¹¹ N. Tsukuda, S. Sugata, H. Saitoh, and Y. Mita, *Appl. Phys. Lett.* **43**, 189 (1983).

¹² G. A. Golubenko, A. M. Prokhorov, V. A. Sychurov, and T. V. Tulakova, *Surfaces* **1**, 88 (1985).

¹³ V. Ya. Panchenko, V. N. Semigonov, and A. I. Khudobenko, Preprint **37**, Center for Sci. Res. on Laser Tech., USSR Acad. Sci., Troisk, 1987; *Kvant. Elektron.* (Moscow) **16**, (1989) [*Sov. J. Quantum Electron.* **19**, (1989)].

¹⁴ D. J. Ehrlich, R. M. Osgood Jr., and T. F. Deutch, *Appl. Phys. Lett.* **39**, 957 (1981).

¹⁵ F. Shaapur and S. D. Allen, *J. Appl. Phys.* **39**, 957 (1981).

¹⁶ V. P. Aksenov and B. G. Zhurkin, Preprint **56**, 194 Phys. Inst. USSR Acad. Sci., Moscow, 1982.

¹⁷ A. M. Prokhorov, V. A. Sychugov, A. V. Tushchenko, and A. A. Khakimov, *Pis'ma Zh. Tekh. Fiz.* **8**, 1409 (1982) [*Sov. Tech. Phys. Lett.* **8**, 605 (1982)].

¹⁸ F. Kielman and Y. H. Bai, *Appl. Phys. A* **29**, 9 (1982).

¹⁹ A. A. Samokhin, V. A. Sychugov, A. V. Tushchenko, and A. A. Khakimov, *Kvant. Elektron.* (Moscow) **10**, 1039 (1983) [*Sov. J. Quantum Electron.* **13**, 659 (1989)].

²⁰ V. N. Anisimov, V. Yu. Baranov, L. A. Bol'shov *et al.*, *Surfaces* **7**, 138 (1983).

²¹ A. M. Prokhorov, A. S. Svakhin, V. A. Sychugov *et al.*, *Kvant. Elektron.* (Moscow) **10**, 906 (1983) [*Sov. J. Quantum Electron.* **13**, 568 (1983)].

²² P. M. Fauchet and A. M. Stegman, *Appl. Phys. A* **32**, 135 (1983).

²³ F. Keilmann, *Surface Studies with Lasers*, F. R. Asseneg, A. Leitner, and M. E. Lippitsh eds. (Springer-Verlag, Berlin, 1983), p. 135.

²⁴ V. V. Bazhenov, A. M. Bonch-Bruevich, M. N. Libenson, and V. S. Makin, *Pis'ma Zh. Tekh. Fiz.* **10**, 1520 (1984) [*Sov. Tech. Phys. Lett.* **10**, 642 (1982)].

²⁵ A. M. Bonch-Bruevich, Ya. A. Imas, G. S. Roanov *et al.*, *Zh. Tekh. Fiz.* **38**, 851 (1968) [*Sov. Phys. Tech. Phys.* **13**, 640 (1968)].

²⁶ T. E. Zavecs, M. A. Safi, and M. Notice, *Appl. Phys. Lett.* **26**, 165 (1975).

²⁷ C. T. Walter and A. H. Clauer, *Appl. Phys. Lett.* **33**, 713 (1978).

²⁸ D. M. Roessler and V. G. Gregson Jr., *Appl. Optics* **17**, 992 (1978).

²⁹ G. M. Gandel'man and P. S. Kondratenko, *Zh. Eksp. Teor. Fiz.* **88**, 1470 (1985) [*Sov. Phys. JETP* **61**, 880 (1985)].

³⁰ V. I. Emil'yanov and V. N. Seminogov, Preprint **15**, Center for Sci. Res. on Laser Tech., USSR Acad. Sci., Troisk, 1987.

³¹ V. V. Kanaev, *Kvant. Elektron.* (Moscow) **14**, 536 (1987) [*Sov. J. Quantum Electron.* **17**, 333 (1987)].

³² P. S. Kondratenko and Yu. N. Orlov, *Kvant. Elektron.* (Moscow) **14**, 1038 (1987) [*Sov. J. Quantum Electron.* **17**, 659 (1987)].

- ³³ L. A. Bol'shov, A. V. Moskovchenko, and M. I. Persiantsev, *Zh. Eksp. Teor. Fiz.* **94**(4), 62 (1988) [*Sov. Phys. JETP* **67**, 683 (1988)].
- ³⁴ P. S. Kondratenko and Yu. N. Orlov, *Surfaces* **8**, 40 (1988).
- ³⁵ N. A. Dunaevskii and V. P. Reshetin, *Dokl. Akad. Nauk Beloruss. SSR* **32**(10), 903 (1988).
- ³⁶ S. I. Anisimov, Ya. A. Imas, G. S. Romanov, and Yu. V. Romanov, *The Effect of High-Power Illumination on Metals*, Nauka, Moscow, 1970.
- ³⁷ V. I. Emil'yanov, E. M. Zemskov and V. N. Seminogov, *Kvant. Elektron. (Moscow)* **10**, 2389 (1983) [*Sov. J. Quantum Electron.* **13**, 1556 (1983)].
- ³⁸ J. F. Young, J. E. Sipe, and H. M. Van Driel, *Opt. Lett.* **8**, 431 (1983).
- ³⁹ *Optical Properties of Semiconductors: A^{III}B^V Compounds*. Willardson and Beer eds., Mir, Moscow, 1970.
- ⁴⁰ V. N. Semigonov and A. I. Khudobenko, Preprint **56**, Center for Sci. Res. on Laser Tech., USSR Acad. Sci., Troisk, 1987.
- ⁴¹ A. M. Dykhne and B. P. Rysev, *Proc. Intl. Sympos. on Surface Waves in Solids and Layered Structures (ISSWAS)*, Vol. 1, p. 29 (Novosibirsk, USSR, 1986).

Translated by Frank J. Crowne